Research Article

Journal of PeptideScience

Received: 7 January 2010 Revised: 25 February 2010 Accepted: 5 March 2010 Published online in Wiley Interscience: 7 May 2010

(www.interscience.com) DOI 10.1002/psc.1234

Double helix formation in α-peptides: a theoretical study

Peter Schramm and Hans-Jörg Hofmann*

A complete overview on all possible hydrogen bonding patterns of double helices with antiparallel and parallel strand orientation in α-peptide sequences is provided on the basis of *ab initio* molecular orbital theory. The most stable representatives belong to the group of antiparallel helices. The study on side chain influence shows that these double helices can only be realized if the strands are composed of L- and D-amino acids in alternate order. The stability of the double helices is compared with that of competing single-stranded helices. The data contribute to an understanding of secondary structure formation in peptides and provide a basis for a rational design of membrane channels. Copyright © 2010 European Peptide Society and John Wiley & Sons, Ltd.

Supporting information may be found in the online version of this article

Keywords: peptide double helices; secondary structure; membrane channels; peptide design; *ab initio* MO theory

Introduction

Double helix formation by association of two conformationally identical native polypeptide strands is a relatively rare event in comparison with nucleic acids and polysaccharides, where it is a characteristic feature. The most prominent example is the peptide antibiotic gramicidin A. This molecule is a sequence of alternating L- and D-amino acids. A single strand with this composition is able to form a mixed or β-helix exhibiting alternate hydrogen-bonded pseudocycles of different size, where the direction of the hydrogen bonds alternately changes in backward and forward directions [1–7]. Two such helices can be arranged in a head-to-head orientation forming a channel through the membrane (Figure 1a). The single-stranded helices show dimer periodicity, i.e. the backbone torsion angles of every second amino acid agree. It was very interesting to see two alternating L,D-polypeptide strands forming double helices as an alternative to the single-stranded helices (Figure 1b and c) [8–19].

In the meantime, several representatives of double helices with L,D-polypeptide strands were experimentally found with both parallel and antiparallel strand orientation (protein data base files: 1MIC [14], 1BDW [16], 1C4D [10,13], and 1AI4 [17]). This finding raises the question on the number of double helix alternatives between peptide strands and their stabilities. In 1977, two groups tried to answer this question on the basis of molecular mechanics [20,21]. They confirmed some of the experimentally available structures and predicted further representatives. However, the range of search was limited in these studies and not all experimentally found structures were confirmed. A detailed look at the data shows that further interaction possibilities have to be considered. In view of the importance of such basic structures for a design of membrane channels, potential antibiotics, and nanomaterials, we decided to perform a more extended systematic search for double helices between α-amino acid strands using the more reliable methods of *ab initio* MO theory.

Methodology

An inspection of the experimentally found double helices shows that the dimer periodicity, which is typical for the single-stranded gramicidin A helices, is kept. As expected, the conformation of the two strands resembles that in β-sheet structures. The interaction mode between the two strands is different in helices with antiparallel and parallel strand orientation. In parallel double helices, an amino acid of one strand interacts with two amino acids of opposite configuration of the other strand via its NH- and CO-functions (Figure 2a). In antiparallel helices, two amino acids of the same configuration in both strands interact pairwise (Figure 2b). On the basis of these interaction modes, all possible hydrogen bonding patterns between two identical peptide strands of approximate β-sheet conformation were generated beginning with the tightest one and continuing up to the three next higher interaction possibilities in the antiparallel case and the two next higher interaction possibilities in the parallel case by using constraints in the geometry optimization. This procedure leads to 11 different hydrogen bonding patterns for antiparallel double helices and 6 different hydrogen bonding patterns for parallel double helices (Tables 1 and 2).

To describe the various interaction patterns in Tables 1 and 2, we numbered the amino acids of the two strands from the *N*- to the *C*-terminus. Now, it is possible to indicate the hydrogen bond patterns considering the dimer periodicity by starting from the NH- and CO-groups of two consecutive amino acids *i* and $(i + 1)$ of the one strand each interacting with the NH- and CO-groups of

* *Correspondence to: Hans-Jörg Hofmann, Institute of Biochemistry, Pharmacy, and Psychology, University of Leipzig, Brüderstraße 34, D-04103 Leipzig, Germany. E-mail: hofmann@uni-leipzig.de*

Institute of Biochemistry, Pharmacy, and Psychology, University of Leipzig, Brüderstraße 34, D-04103 Leipzig, Germany

Journal of PeptideScience

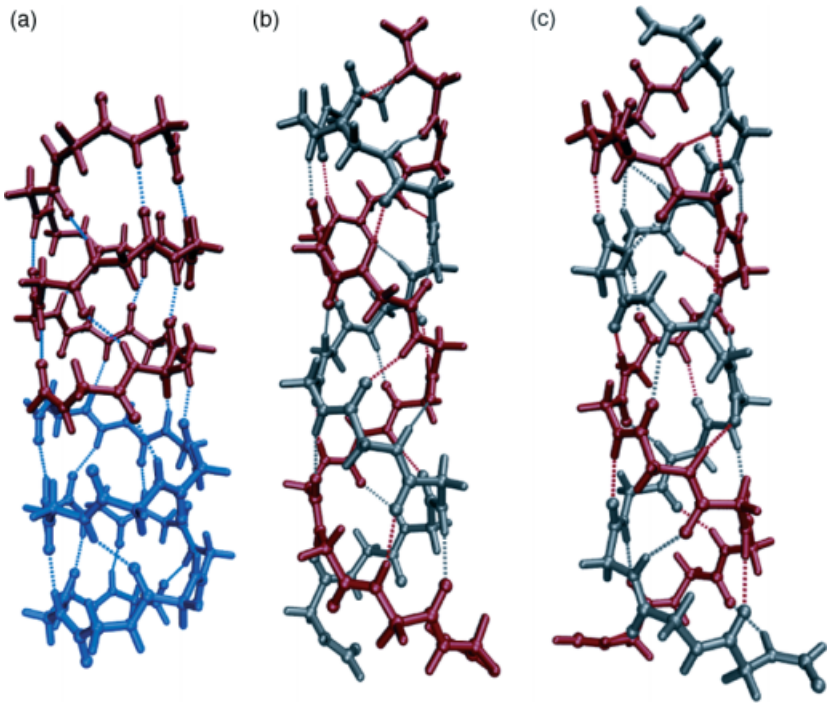

Figure 1. Gramicidin A-like helices: (a) two single-stranded helices in head-to-head arrangement; (b) double helix with antiparallel strand orientation; and (c) double helix with parallel strand orientation.

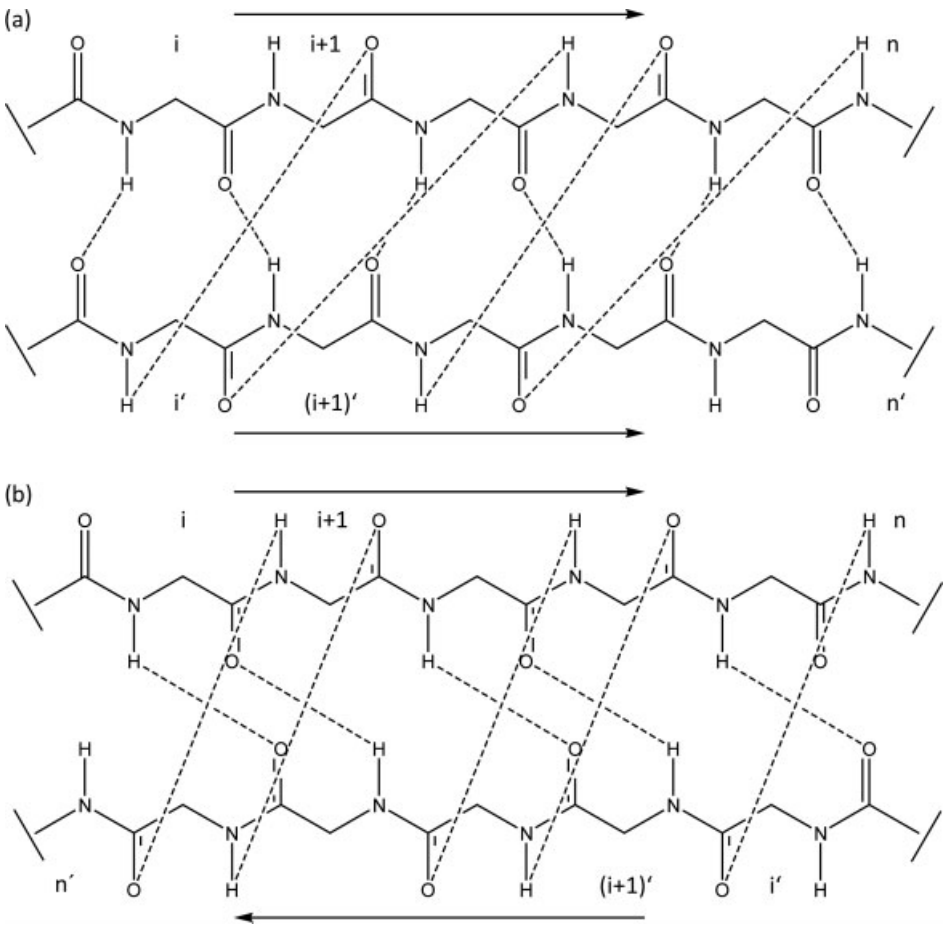

Figure 2. Hydrogen bonding principles in: (a) the tightest double helix with parallel orientation of two poly-glycine strands and (b) the tightest double helix with antiparallel orientation of two poly-glycine strands.

Table 1. Overview on the formally possible hydrogen bonding patterns in double helices with antiparallel strand orientation[a,b]

1	*i*NH → (*n* − *i*)′CO (*n* − *i*)′NH → *i*CO (*i* + 1)NH → (*n* − *i* + 1)′CO (*n* − *i* + 1)′NH → (*i* + 1)CO	**2**	*iNH* → (*n* − *i*)′*CO* (*n* − *i*)′*NH* → *iCO* (*i* + 1)*NH* → (*n* − *i* + 3)′*CO* (*n* − *i* + 3)′*NH* → (*i* + 1)*CO*	**3**	***i*NH** →(***n*** − ***i***)′**CO** (***n*** − ***i***)′**NH** →***i*CO** (***i*** + **1)NH** →(***n*** − ***i*** + **5)′CO** (***n*** − ***i*** + **5)′NH** →(***i*** + **1)CO**[b]
4	***iNH*** → ***(n*** − ***i*** − **1)′*CO*** ***(n*** − ***i*** − **1)′*NH*** →***iCO*** ***(i*** + **1)*NH*** →***(n*** − ***i*** + **1)′*CO*** ***(n*** − ***i*** + **1)′*NH*** →***(i*** + **1)*CO***[c]	**5**	***iNH*** →***(n*** − ***i*** − **1)′*CO*** ***(n*** − ***i*** − **1)′*NH*** →***iCO*** ***(i*** + **1)*NH*** →***(n*** − ***i*** + **3)′*CO*** ***(n*** − ***i*** + **3)′*NH*** →***(i*** + **1)*CO***[d]		
6	*i*NH → (*n* − *i* − 3)′CO (*n* − *i* − 3)′NH →iCO (*i* + 1)NH → (*n* − *i* + 1)′CO (*n* − *i* + 1)′NH → (*i* + 1)CO	**7**	*i*NH → (*n* − *i* − 3)′CO (*n* − *i* − 3)′NH → *i*CO (*i* + 1)NH → (*n* − *i* + 3)′CO (*n* − *i* + 3)′NH → (*i* + 1)CO		
8	*iNH* → (*n* − *i* − 5)′*CO* (*n* − *i* − 5)′*NH* → *iCO* (*i* + 1)*NH* → (*n* − *i* + 1)′*CO* (*n* − *i* + 1)′*NH* → (*i* + 1)*CO*	**9**	*iNH* → (*n* − *i* − 5)′*CO* (*n* − *i* − 5)′*NH* → *iCO* (*i* + 1)*NH* → (*n* − *i* + 3)′*CO* (*n* − *i* + 3)′*NH* → (*i* + 1)*CO*		
10	*i*NH → (*n* − *i* − 7)′CO (*n* − *i* − 7)′NH → *i*CO (*i* + 1)NH → (*n* − *i* + 1)′CO (*n* − *i* + 1)′NH → (*i* + 1)CO	**11**	*iNH* → (*n* − *i* − 7)′*CO* (*n* − *i* − 7)′*NH* → *iCO* (*i* + 1)*NH* → (*n* − *i* + 3)′*CO* (*n* − *i* + 3)′*NH* → (*i* + 1)*CO*		

[a] $n = n'$, number of amino acids per strand; *i*, *i*′, amino acid positions on the stands 1 and 2; helix patterns experimentally found in bold, helix patterns found by molecular mechanics in italics, helix patterns found both in experiment and by molecular mechanics in bold and italics.
[b] PDB-code: 1BDW [16].
[c] PDB-code: 1Al4 [17].
[d] PDB-code: 1C4D [10,13].

Table 2. Overview on the formally possible hydrogen bonding patterns in double helices with parallel strand orientation[a]

12	*i*NH → (*i* − 1)′CO (*i* + 1)′NH → *i*CO (*i* + 1)NH → (*i* − 2)′CO *i*′NH → (*i* + 1)CO	**13**	*i*NH → (*i* − 1)′CO (*i* + 1)′NH → *i*CO (*i* + 1)NH → (*i* − 4)′CO (*i* − 2)′NH → (*i* + 1)CO
14	***iNH*** →***(i*** + **1)′*CO*** ***(i*** + **3)′*NH*** →***iCO*** ***(i*** + **1)*NH*** →***(i*** − **2)′*CO*** ***i*′*NH*** →***(i*** + **1)*CO***[b]	**15**	*i*NH → (*i* + 1)′CO (*i* + 3)′NH → *i*CO (*i* + 1)NH → (*i* − 4)′CO (*i* − 2)′NH → (*i* + 1)CO
16	*iNH* → (*i* + 3)′*CO* (*i* + 5)′*NH* → *iCO* (*i* + 1)*NH* → (*i* − 2)′*CO* *i*′*NH* → (*i* + 1)*CO*	**17**	*i*NH → (*i* + 3)′CO (*i* + 5)′NH → *i*CO (*i* + 1)NH → (*i* − 4)′CO (*i* − 2)′NH → (*i* + 1)CO

[a] $n = n'$, number of amino acids per strand; *i*, *i*′, amino acid positions on the stands 1 and 2; helix patterns experimentally found in bold; helix patterns found by molecular mechanics in italics, helix patterns found both in experiment and in molecular mechanic studies in bold and italics.
[b] PDB-code: 1MIC [14].

amino acids of the other strand following the general interaction principles for parallel and antiparallel double helices described earlier and illustrated in Figure 2. The positions of the interacting amino acids on the second strand are indicated by a prime. In our calculations, the strands consisted of 14 amino acids ($n = n' = 14$) blocked by an acetyl group at the *N*- and an NHMe-group at the *C*-terminus.

The double helices obtained in the constrained geometry optimization were subject of free geometry optimization then by deleting the constraints followed by an inspection of the backbone structure to check the maintenance of the dimer periodicity and the hydrogen bond pattern. Finally, the minimum character of the optimized structures was confirmed by the calculation of the vibration frequencies. These calculations provided also the free enthalpy differences between the various double helices.

To get a complete overview on all principal double helix possibilities, side chains were omitted at first. The poly-glycine double helices obtained in this way provided the basis for an estimation of side chain effects extending the study to poly-alanine double helices.

All calculations were performed at the Hartree–Fock level of *ab initio* molecular orbital (MO) theory selecting the 6-31G* basis set (HF/6-31G*) and using the Gaussian 03 program package [22]. In numerous studies, the HF/6-31G* approximation level has proved to be reliable for the prediction of structural and energetic data of peptide secondary structures [6,23–27]. In view of the considerable size of the double helices with 14 amino acid residues per strand, it is an acceptable approximation level for complete geometry optimizations and the calculation of the vibration frequencies.

Results and Discussion

Helix Types

The complete geometry optimization and the analysis of the vibration frequencies confirm all 11 antiparallel and 5 of the 6 parallel double helix patterns in Tables 1 and 2 as minimum conformations for poly-glycine strands. The hydrogen bonding pattern **12** with parallel strand orientation (Table 2) is not kept in the geometry optimization. The conformation of the two strands is rather extended in this structure and excludes a regular hydrogen bonding. The relative energies and free enthalpies of the various

Journal of PeptideScience

Table 3. Relative energies[a] and free enthalpies[a] of poly-glycine and poly-L,D-alanine double helices with parallel and antiparallel strand orientations at the HF/6-31G* level of *ab initio* MO theory

	ΔE		ΔG
Helix type[b]	Poly-glycine	Poly-L,D-alanine	Poly-glycine
Antiparallel strands			
1	239.3	322.4	191.7
2	**0.0**[c]	15.5	3.1
3	13.4	**0.0**[d]	1.9
4	16.8	18.5	31.7
5	3.9	6.9	15.3
6	34.0	68.5	15.3
7	19.2	64.5	**0.0**[e]
8	25.2	38.4	3.7
9	50.2	75.1	4.9
10	53.2	62.2	4.4
11	69.9	123.1	2.8
Parallel strands			
13	29.8	34.5	29.9
14	16.5	18.5	34.4
15	41.4	56.1	37.3
16	34.0	35.9	34.6
17	47.4	97.9	39.9

[a] Relative energies and free enthalpies are expressed in kJ/mol.
[b] See Tables 1 and 2.
[c] $E_T = -5871.419101$ a.u.
[d] $E_T = -6886.397742$ a.u.
[e] $E_T = -5869.773693$ a.u.

Table 4. Average backbone torsion angles[a] of a dimer unit of poly-glycine double helices at the HF/6-31G* level of *ab initio* MO theory

Helix type[b]	φ_i	ψ_i	φ_{i+1}	ψ_{i+1}
Antiparallel strands				
1	−93.0	168.1	171.4	−141.5
2	−95.8	146.2	155.2	−125.7
3	−117.2	145.3	149.6	−134.3
4	−99.1	143.1	154.8	−124.8
5	−116.6	138.0	149.0	−136.5
6	−114.1	137.8	144.8	−143.1
7	−131.9	146.8	132.9	−136.5
8	−111.7	122.7	153.5	−157.7
9	−136.8	146.8	152.7	−155.0
10	−127.2	132.7	157.7	−161.4
11	−147.1	154.6	159.0	−153.0
Parallel strands				
13	−84.0	142.4	149.9	−133.1
14	−104.3	145.4	150.9	−114.9
15	−119.4	145.1	135.7	−116.9
16	−118.4	141.2	143.1	−126.3
17	−105.7	140.0	160.9	−108.3

[a] Backbone torsion angles are expressed in degrees; for complete geometry information, see supporting information.
[b] See Tables 1 and 2.

double helices are given in Table 3. The average backbone torsion angles corresponding to the dimer periodicity are listed in Table 4. The complete geometry information is provided in the supporting information. It can be seen that the most stable representatives belong to the group of antiparallel helices. This corresponds to the situation in parallel and antiparallel β-sheet structures. The most stable double helix pattern **2** has not been found in experiments until now. The four experimentally found double helices **3**–**5** with antiparallel strand orientation and **14** with parallel strand orientation are less unstable and follow in the stability order (Table 3). There is a fair agreement between the theoretically estimated and the experimental geometries. The hydrogen bonds in all predicted structures are approximately linear. The CO···HN distances are in between 2.05 and 2.27 Å. In Figures 3 and 4, all antiparallel and parallel double helices formed between two poly-glycine strands are visualized. It can be seen that the lengths of the double helices decrease, whereas their diameters increase, the further interacting peptide bonds are distant in the sequence.

Side Chain Effects

The pool of poly-glycine double helices provides a good basis for an estimation of side chain influences. Therefore, alanine side chains were added to these structures followed by complete geometry optimizations. All attempts to maintain regular double helices with only D- or, alternatively, L-configured alanines failed. Thus, the poly-glycine double helix patterns could only be obtained in poly-alanine sequences of alternating D- and L-amino acids. There are some changes in the stability order (Table 3). The antiparallel double helix **3**, which was also experimentally found, is most stable now followed by the double helix **5**, which is also known from experiment. Only then, the most stable hydrogen bonding pattern **2** of the poly-glycine double helices appears. It should be mentioned that the most stable double helix **3** was not found on the basis of the molecular mechanics calculations. The average backbone torsion angles of all poly-alanine double helices are given in Table 5. They fairly agree with those of the poly-glycine double helices (Table 4). The complete geometry information on the poly-alanine helices is available in the supporting information.

Competition Between Single- and Double-Stranded Helices

It could be interesting to discuss the competition of the double helix structures with the single-stranded gramicidin A-like helices. In the single-stranded helices, 20- and 22-membered hydrogen-bonded pseudocycles alternate, but helices with alternating 14- and 16-membered pseudocycles are also possible [4–6,18,19]. By geometry optimization of the single-stranded L,D-polyalanine helices corresponding in length and configuration to the two strands of the double helices at the same level of theory, it was possible to estimate the stability difference between double helices and two alternative single-stranded helices. In Table 6, the data are given for the most stable antiparallel and parallel double helices. It can be seen that the formation of double helices is intrinsically favored over the formation of single-stranded helices with 20/22- or 14/16-alternation of the hydrogen-bonded pseudocycles in vacuum, which indicates that they may be realized as channels in a polar environment of a membrane. The rank order changes considerably in a polar medium. An estimation of the influence of a polar solvent on the stability of the single-stranded and the most stable double helices using a polarizable continuum model (PCM) [28] at the IEFPCM//HF/6-31G* level

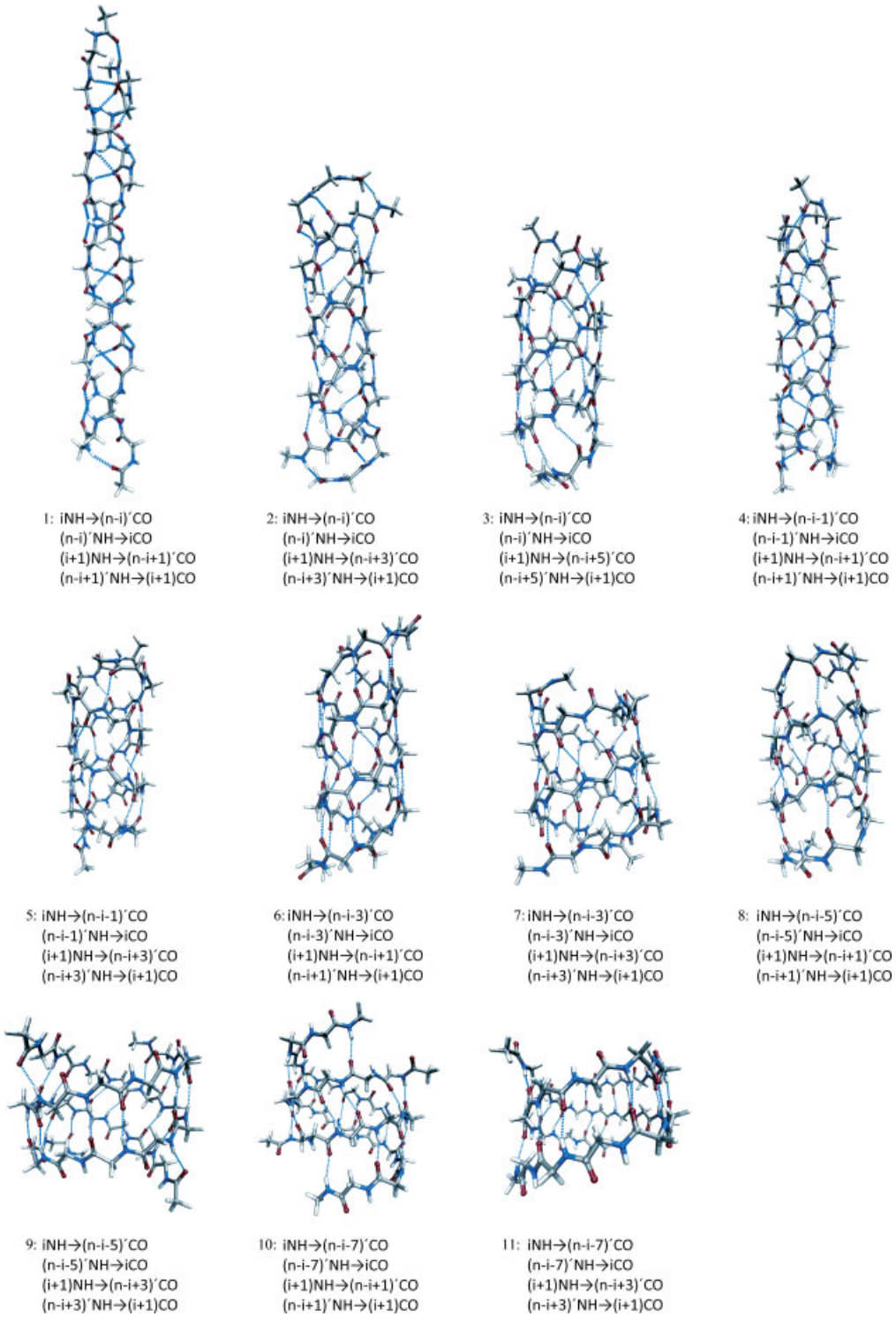

Figure 3. Theoretically predicted antiparallel double helices between two poly-glycine strands ($n = n' = 14$) obtained at the HF/6-31G* level of *ab initio* MO theory.

of *ab initio* MO theory (dielectric constant for water, $\varepsilon = 78.4$) shows that the single-stranded helices gain considerable stability in this environment. Referred to the 16/14-single-stranded helix, the most stable antiparallel and parallel double helices **3, 5**, and **16** are still more stable, but referred to the 22/20-single-stranded gramicidin A helix, the double helices are energetically disadvantaged (Table 6).

Conclusion

On the basis of *ab initio* MO theory, it was possible to provide an overview on the possibilities of double helix formation in sequences of α-peptides. Both the representatives of antiparallel and parallel double helices were found with poly-glycine strands. The most stable double helices have an antiparallel orientation

Journal of PeptideScience

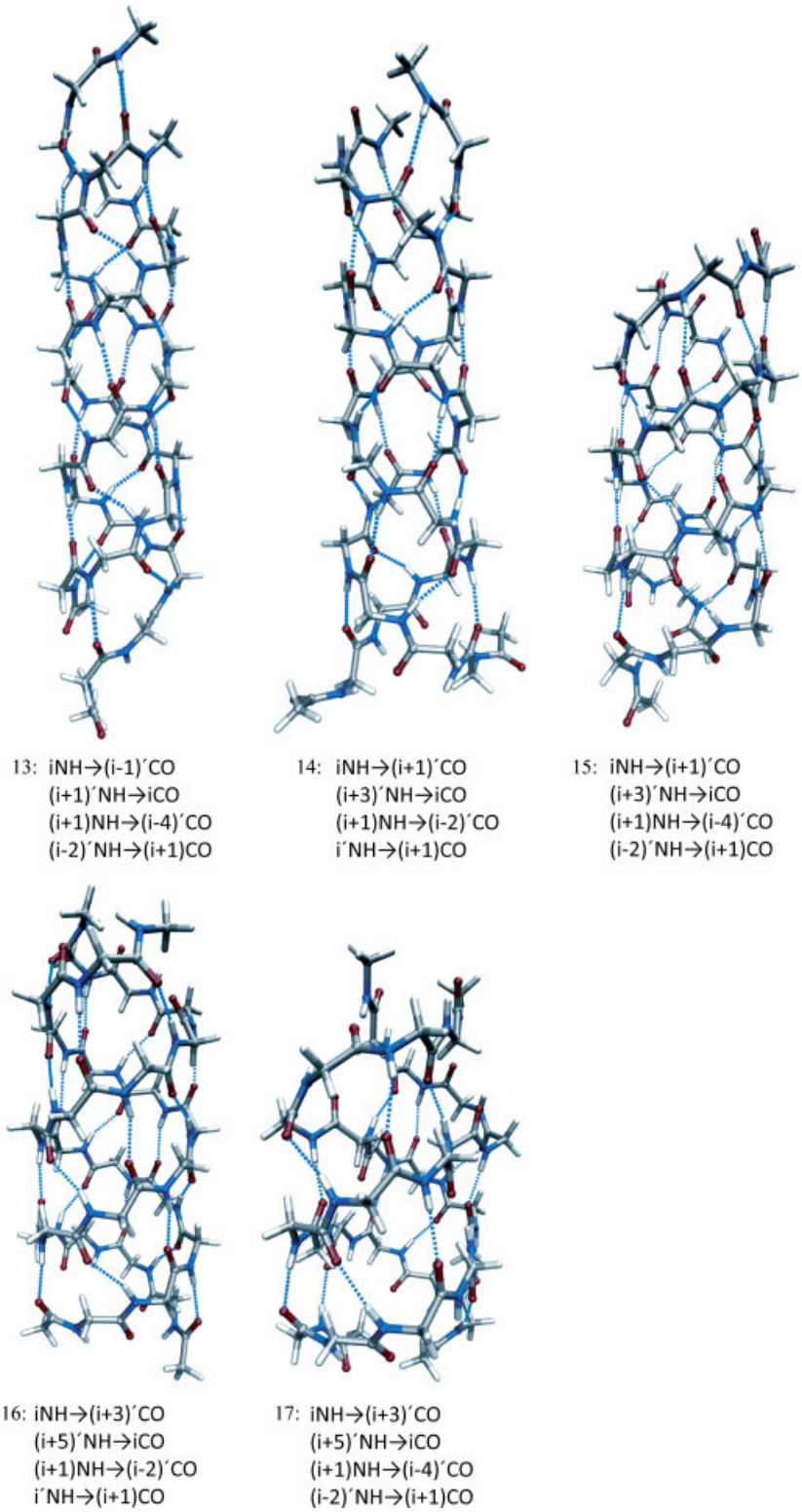

Figure 4. Theoretically predicted parallel double helices between two poly-glycine strands ($n = n' = 14$) obtained at the HF/6-31G* level of *ab initio* MO theory.

of the two strands. All hydrogen bond patterns could also be confirmed for poly-alanine strands, but only with alternating L- and D-alanine constituents. Strands with amino acids of identical configuration cannot maintain regular structures. The two poly-alanine double helices predicted as most stable by theory were also found in experimental studies. The intrinsic stability of poly-alanine double helices is higher than that of single-stranded helix alternatives of gramicidin A type, but in a polar environment this changes in favor of the single-stranded helices. The numerous double helix patterns suggested

Table 5. Average backbone torsion angles[a] of a dimer unit of poly-L,D-alanine double helices ($n = n' = 14$) at the HF/6-31G* level of *ab initio* MO theory

Helix type[b]	φ_L	ψ_L	φ_D	ψ_D
Antiparallel strands				
1	−93.4	166.8	173.3	−140.4
2	−104.5	141.4	156.8	−123.5
3	−125.2	139.8	157.1	−131.7
4	−101.5	137.9	156.8	−123.8
5	−118.4	141.6	151.8	−132.2
6	−114.3	137.4	152.0	−134.8
7	−137.6	144.5	155.3	−146.8
8	−133.5	142.1	155.0	−145.8
9	−137.1	149.1	155.7	−148.5
10	−145.8	147.3	156.5	−149.5
11	−153.7	152.2	157.9	−156.4
Parallel strands				
13	−124.2	146.9	149.2	−94.9
14	−107.0	142.2	152.7	−111.9
15	−117.1	140.1	148.9	−131.7
16	−132.2	139.9	149.0	−120.3
17	−132.3	142.3	148.9	−138.2

[a] Backbone torsion angles are expressed in degrees; for complete geometry information, see supporting information.
[b] See Tables 1 and 2.

Table 6. Energy differences[a] between the most stable poly-L,D-alanine double helices and two single strands of gramicidin A-like helices with alternating 16- and 14-[b] and 22- and 20-membered[b] hydrogen-bonded pseudocycles in vacuum (HF/6-31G*) and in aqueous solution (IEFPCM//HF/6-31G*)

	$Helix_{16/14}$		$Helix_{22/20}$	
Helix type[c]	ΔE_T	ΔE_T (PCM)	ΔE_T	ΔE_T (PCM)
Antiparallel strands				
2	−105.2	15.9	−103.4	69.4
3	−120.7	−28.2	−118.9	25.3
4	−102.2	5.7	−100.5	59.2
5	−113.8	−37.4	−112.0	16.1
Parallel strands				
13	−86.2	4.8	−84.4	58.3
14	−102.2	6.9	−100.4	60.4
16	−84.8	−20.9	−83.0	32.5

[a] Energy differences are expressed in kJ/mol.
[b] For total energies of single- and double-stranded helices in vacuum and in aqueous solution, see supporting information.
[c] See Tables 1 and 2.

represent a good basis for a rational design of membrane channel structures.

Acknowledgement

This work was supported by Deutsche Forschungsgemeinschaft (Project HO 2346/1-3 and SFB 610).

Supporting information

Supporting information may be found in the online version of this article.

References

1 Urry DW. The gramicidin A transmembrane channel: a proposed π(L,D) helix. *Proc. Natl. Acad. Sci. U. S. A.* 1971; **68**: 672–676.
2 Urry DW, Goodall MC, Glickson JD, Mayers DF. The gramicidin A transmembrane channel: characteristics of head-to-head dimerized π (L,D) helices. *Proc. Natl. Acad. Sci. U. S. A.* 1971; **68**: 1907–1911.
3 Kovacs F, Quine J, Cross TA. Validation of the single-stranded channel conformation of gramicidin A by solid-state NMR. *Proc. Natl. Acad. Sci. U. S. A.* 1999; **96**: 7910–7915.
4 Ramachandran GN, Chandrasekaran R. Conformation of peptide chains containing both L-residues and D-residues. 1. Helical structures with alternating L-residues and D-residues with special reference to LD-ribbon and LD-helices. *Indian J. Biochem. Biophys.* 1972; **9**: 1–11.
5 De Santis P, Morosetti S, Rizzo R. Conformational analysis of regular enantiomeric sequences. *Macromolecules* 1974; **7**: 52–58.
6 Baldauf C, Günther R, Hofmann HJ. Mixed helices – a general folding pattern in homologous peptides? *Angew. Chem. Int. Ed.* 2004; **43**: 1594–1597.
7 Yashima E, Maeda K, Furusho Y. Single- and double-stranded helical polymers: synthesis, structures, and functions. *Acc. Chem. Res.* 2008; **41**: 1166–1180.
8 Lotz B, Colonna-Cesari F, Heitz F, Spach G. Family of double helices of alternating poly(gamma-benzyl-D-L-glutamate). A stereochemical model for gramicidin-A. *J. Mol. Biol.* 1976; **106**: 915–942.
9 Lorenzi GP, Jäckle H, Tomasic L, Rizzo V, Pedone C. Linear stereocooligopeptides with alternating D- and L-residues. 3. Nature and relative stability of monomeric and dimeric species of the D,L-alternating octapeptide Boc-(L-Val-D-Val)$_4$-OMe in cyclohexane or chloroform solution. *J. Am. Chem. Soc.* 1982; **104**: 1728–1733.
10 Wallace BA, Ravikumar K. The gramicidin pore – crystal structure of a cesium complex. *Science* 1988; **241**: 182–187.
11 Di Blasio B, Benedetti E, Pavone V, Pedone C. Regularly alternating L,D-peptides. 2. The double-stranded right-handed antiparallel β-helix in the structure of tert-Boc-(L-Phe-D-Phe)$_4$-OMe. *Biopolymers* 1989; **28**: 203–214.
12 Fenude E, Tomasic L, Lorenzi GP. Conformationally constrained D,L-alternating oligopeptides. *Biopolymers* 1989; **28**: 185–192.
13 Wallace BA, Hendrickson WA, Ravikumar K. The use of single-wavelength anomalous scattering to solve the crystal structure of a gramicidin A cesium chloride complex. *Acta Crystallogr. B* 1990; **46**: 440–446.
14 Chen Y, Tucker A, Wallace BA. Solution structure of a parallel left-handed double-helical gramicidin-A determined by 2D ^{1}H NMR. *J. Mol. Biol.* 1996; **264**: 757–769.
15 Wallace BA. Recent advances in the high resolution structures of bacterial channels: gramicidin A. *J. Struct. Biol.* 1998; **121**: 123–141.
16 Burkhart BM, Li N, Langs DA, Pangborn, WA, Duax WL. The conducting form of gramicidin A is a right-handed double-stranded double helix. *Proc. Natl. Acad. Sci. U. S. A.* 1998; **95**: 12950–12955.
17 Burkhart BM, Gassman RM, Langs DA, Pangborn WA, Duax WL. Heterodimer formation and crystal nucleation of gramicidin D. *Biophys. J.* 1998; **75**: 2135–2146.
18 Navarro E, Fenude E, Celda B. Solution structure of a D,L-alternating oligonorleucine as a model of double-stranded antiparallel β-helix. *Biopolymers* 2002; **64**: 198–209.
19 Navarro E, Fenude E, Celda B. Conformational and structural analysis of the equilibrium between single- and double-strand β-helix of a D,L-alternating oligonorleucine. *Biopolymers* 2004; **73**: 229–241.
20 Venkatram Prasad BV, Chandrasekaran R. Conformation of polypeptide chains containing both L- and D-residues. *Int. J. Pept. Protein Res.* 1977; **10**: 129–138.
21 Colonna-Cesari F, Premilat S, Heitz F, Spach G, Lotz B. Helical structures of poly(D-L-peptides). A conformational energy analysis. *Macromolecules* 1977; **10**: 1284–1288.
22 Frisch MJ, Trucks GW, Schlegel HB, Scuseria GE, Robb MA, Cheeseman JR, Montgomery JA, Vreven T, Kudin KN, Burant JC,

Millam JM, Iyengar SS, Tomasi J, Barone V, Mennucci B, Cossi M, Scalmani G, Rega N, Petersson GA, Nakatsuji H, Hada M, Ehara M, Toyota K, Fukuda R, Hasegawa J, Ishida M, Nakajima T, Honda Y, Kitao O, Nakai H, Klene M, Li X, Knox JE, Hratchian HP, Cross JB, Adamo C, Jaramillo J, Gomperts R, Stratmann RE, Yazyev O, Austin AJ, Cammi R, Pomelli C, Ochterski JW, Ayala PY, Morokuma K, Voth GA, Salvador P, Dannenberg JJ, Zakrzewski VG, Dapprich S, Daniels AD, Strain MC, Farkas O, Malick DK, Rabuck AD, Raghavachari K, Foresman JB, Ortiz JV, Cui Q, Baboul AG, Clifford S, Cioslowski J, Stefanov BB, Liu G, Liashenko A, Piskorz P, Komaromi I, Martin RL, Fox DJ, Keith T, Al-Laham MA, Peng CY, Nanayakkara A, Challacombe M, Gill PMW, Johnson B, Chen W, Wong MW, Gonzalez C, Pople JA. *Gaussian 03, Revision C.02*. Gaussian Inc.: Wallingford, CT, 2004.

23 Head-Gordon T, Head-Gordon M, Frisch MJ, Brooks CL III, Pople JA. Theoretical study of blocked glycine and alanine peptide analogs. *J. Am. Chem. Soc.* 1991; **113**: 5989–5997.

24 Endredi G, Perczel A, Farkas O, McAllister MA, Csonka GI, Ladik J, Csizmadia IG. Peptide models XV. The effect of basis set size increase and electron correlation on selected minima of the ab initio 2D-Ramachandran map of For-Gly-NH_2 and For-L-Ala-NH_2. *J. Mol. Struct. (Theochem)* 1997; **391**: 15–26.

25 Rommel-Möhle K, Hofmann HJ. Conformation dynamics in peptides: quantum chemical calculations and molecular dynamics simulations on *N*-acetylalanyl-*N*′-methylamide. *J. Mol. Struct. (Theochem)* 1993; **285**: 211–219.

26 Möhle K, Gussmann M, Rost A, Cimiraglia R, Hofmann HJ. Correlation energy, thermal energy, and entropy effects in stabilizing different secondary structures of peptides. *J. Phys. Chem. A* 1997; **101**: 8571–8574.

27 Möhle K, Hofmann HJ, Thiel W. Description of peptide and protein secondary structures employing semiempirical methods. *J. Comput. Chem.* 2001; **22**: 509–520.

28 Tomasi J, Mennucci B, Cammi R. Quantum mechanical continuum solvation models. *Chem. Rev.* 2005; **105**: 2999–3094.

